A Redox-Dependent Electrochromic Material: *Tetri*-EDOT Substituted Thieno[3,2-*b*]thiophene

Jingjing Shi, Xiaosi Zhu, Panpan Xu, Mengmeng Zhu, Yitong Guo, Yaowu He, Zhao Hu, Imran Murtaza, Hongtao Yu, Lijia Yan, Osamu Goto, Hong Meng*

Organic electrochromic materials change color rapidly under applied potential. A butterfly-shaped compound, 5,5′,-5″,-5‴-(thieno[3,2-*b*]thiophene-2,3,5,6-tetrayl) tetrakis-(2,3-dihydrothieno[3,4-*b*][1,4]dioxine) (t-EDOT-TT) is synthesized for the first time and polymerized at different potentials via electropolymerization technique. By applying different polymerization potentials, the optical and electrochromic properties of this newly synthesized polymer can be tuned. Owing to the dependence of functional group position in the polymer structure on the redox potential, this polymer can be utilized in very interesting organic optoelectronic applications.

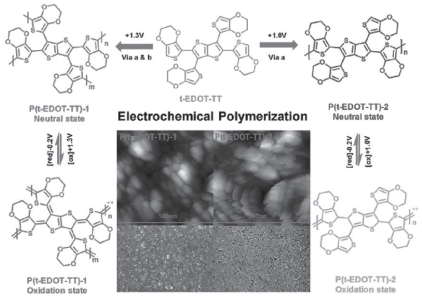

1. Introduction

Electrochromic materials (ECs) are an important class of conducting polymers which change their optical properties in response to the alteration in applied potential. After the discovery of first electrochromic material in 1960s[1] and development of the conducting polymers in 1970s,[2] there has been a tremendous growth in the field of electrochromism. Since then electrochromic conducting polymers, which are classified as organic electrochromic (OEC) materials received great attention due to their numerous merits over inorganic materials such as having fast response time, flexibility, ease of device fabrication, facile chemical modification, a relatively narrow absorption band in displaying diverse and clear color, large-scale processability, and being light weight.[3–5] There are many interesting applications of OEC materials such as, smart windows,[6] flexible displays,[7,8] electrochromic fibers,[6,9] sunglasses,[10] supercapacitors,[11,12] and so on. When a suitable electric potential is applied an EC material changes its color as a result of redox processes at different potentials.[13] Complementary colors are generally given by the polymer due to selective absorption and reflection of different wavelengths of light upon changing the applied voltage.[14] While a variety of materials have been investigated as active electrochromic materials, by applying redox potential to polymerize, the extent to which the change in electrochromic properties of a polymerized material can be achieved by applying different voltages has not been elucidated. The potential for such materials may be used for unique practical applications, where redox modulation is required. With this in mind, herein we report a new approach to design

J. Shi, X. Zhu, P. Xu, M. Zhu, Y. Guo, Dr. Y. He, Z. Hu, Prof. O. Goto, Prof. H. Meng
School of Advanced Materials
Peking University Shenzhen Graduate School
Shenzhen 518055, China
E-mail: menghong@pkusz.edu.cn
Dr. I. Murtaza, Dr. H. Yu, L. Yan, Prof. H. Meng
Key Laboratory of Flexible Electronics (KLOFE)
& Institute of Advanced Materials (IAM)
Jiangsu National Synergetic Innovation Center for Advanced Materials (SICAM)
Nanjing Tech University (Nanjing Tech)
30 South Puzhu Road, Nanjing 211816, China

Macromol. Rapid Commun. **2016**, DOI: 10.1002/marc.201600157

redox-dependent monomers whose electrochromic properties can be tuned by the applied voltage. The idea of this approach combines the widely investigated electrochemically active monomer EDOT and the easily chemically modified thieno[3,2-*b*]thiophene moiety. Thieno[3,2-*b*]-thiophene based organic and polymeric materials have been studied in the application of organic photovoltaic, organic light emitting diodes and especially thieno[3,2-*b*]-thiophene fused with phenyl materials have shown high charge mobilities in organic thin film transistors (OTFTs).[15–17] On the other hand, a myriad of electrochromic polymers based on EDOT has been widely investigated. To the best of our knowledge, very few reports elucidate multi-EDOT substituted thieno[3,2-*b*]thiophene series as organic electrochromic materials. It is known that thieno[3,2-*b*]thiophene unit has intrinsic rigidity[18] due to the strong S—S and S—C interaction forces and by adding EDOT, π–π stacking increases which has a significant effect on the band gap, which makes a strong influence on the absorption spectrum of the compound. In this work, therefore, we designed and synthesized 5,5′,-5″,-5‴-(thieno[3,2-*b*]thiophene-2,3,5,6-tetrayl)tetrakis-(2,3-dihydrothieno [3, 4-*b*][1,4]dioxine) (t-EDOT-TT), polymerized at 2,5 and 2,5,3,6 EDOT and explored its electrochromic properties.

2. Experimental Section

2.1. Synthesis

Scheme 1 shows the synthetic strategy of the monomer. t-EDOT-TT was synthesized by dissolving compound Perbromothieno[3,2-*b*]thiophene (1.64 g, 3.63 mmol) and compound Tributyl(2,3-dihydrothieno[3,4-*b*][1,4]dioxin-5-yl)stannane (9.1 g, 21.0 mmol) in dry THF (200 mL). The solution was purged with argon for 30 min and $PdCl_2(PPh_3)_2$ (0.673 g, 0.96 mmol, 26.3%) was added at room temperature. The mixture was then stirred at 100 °C under argon atmosphere for 20 h before cooling it down to room temperature. After removing the solvent, the residue was subjected to silica gel chromatography (PE:DCM = 1:2) to finally obtain t-EDOT-TT monomer in the form of a light yellow powder with isolated yield 30%. EI, MS mz (%): 700 (100, M+) ^{1}H NMR (300 MHz, $CDCl_3$) δ 6.53 (s, 2H), 6.23(s, 2H), 4.21 (dd, 16H). ^{13}C NMR (300 MHz, DMSO): δ (ppm) 142.0, 141.1, 140.5, 139.6, 133.3, 118.8, 110.3, 107.2, 101.5, 100.9, 65.4, 64.5. Initially testing different coupling reaction methods, including Suzuki-coupling[19] and Grignard coupling with low yield, we finally successfully synthesized the target product via Stille coupling[20] method to give a separated yield of 30%.

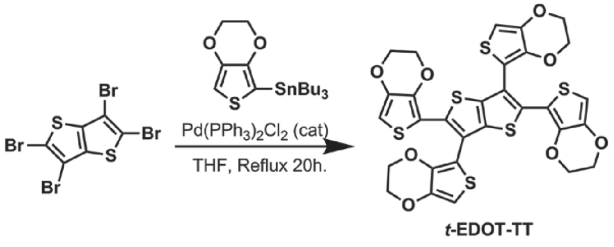

Scheme 1. Synthesis of t-EDOT-TT via Stille coupling.

2.2. Electrochemical Polymerization

The chemical structure of the monomer characterized by ^{1}H NMR gives direct evidence of different C—H substituted EDOT, clearly indicating the availability of two reaction sites. ^{1}H NMR of position **a** is 6.23 ppm, while that of position **b** is 6.53 ppm, which shows that the chemical shift of **a** is lower than **b**. Moreover, from Gaussian software calculations (Figure S1, Supporting Information), we found that the electron density of **a** is higher than **b**, thus **a** can lose electrons more easily to become radical cation (Figure S2, Supporting Information), which implies that site **a** is more electrophilic as compared to site **b**.[21,22] The polymerization at **a** forms a more conjugated structure with higher electron density, therefore, the electropolymerization of **a** can be achieved at lower applied potential as compared to **b** (Scheme 2)[23] and **a–a** connection is relatively easier than the **b–b** connection. In addition, there is a steric hindrance which prevents **b–b** connection before **a–a** connection. So at +1.0 V **a–a** connection is more suitable, whereas at +1.3 V **a–a** connection is initiated before the **b–b** connection. From Raman spectra (Figure S3, Supporting Information), we can see that the polymers synthesized at +1.3 and +1.0 V are quite different from each other and the polymer P(t-EDOT-TT)-1 which was electropolymerized at +1.3 V also shows fluorescence phenomenon.

All electrochemical tests and polymerizations were performed in a three electrode cell with indium tin oxide (ITO) coated glass as the working electrode, Pt as the counter electrode and Ag as the pseudo reference electrode. Polymer thin films were deposited on ITO by oxidative electropolymerization in a dichloromethane (DCM) solution containing 0.56×10^{-3} M monomer and 0.1 M tetrabutylammonium hexafluorophosphate ($TBAPF_6$). The representative electrochemical growth process of monomers t-EDOT-TT to form corresponding polymers is shown in Scheme 2.

3. Results and Discussion

To examine the redox difference, we conducted step-potential CV scans and observed a red-brown polymer, P(t-EDOT-TT)-1, obtained at higher applied potential. While at lower applied potential, a blue polymer, P(t-EDOT-TT)-2 was formed. This change is attributed to the two different reaction sites, suggesting that the monomer can be electrochemically polymerized at two different applied voltages to generate two different electrochromic polymers due to the conformational structural change.

The monomer was polymerized potentiodynamically on ITO coated glass slide. The cyclic voltammograms for electrochemical polymerization of the monomers at a scan rate of 100 mV s^{-1} are depicted in Figure 1. As observed in other electrochemical polymerization processes, in the

Macromol. Rapid Commun. **2016**, DOI: 10.1002/marc.201600157

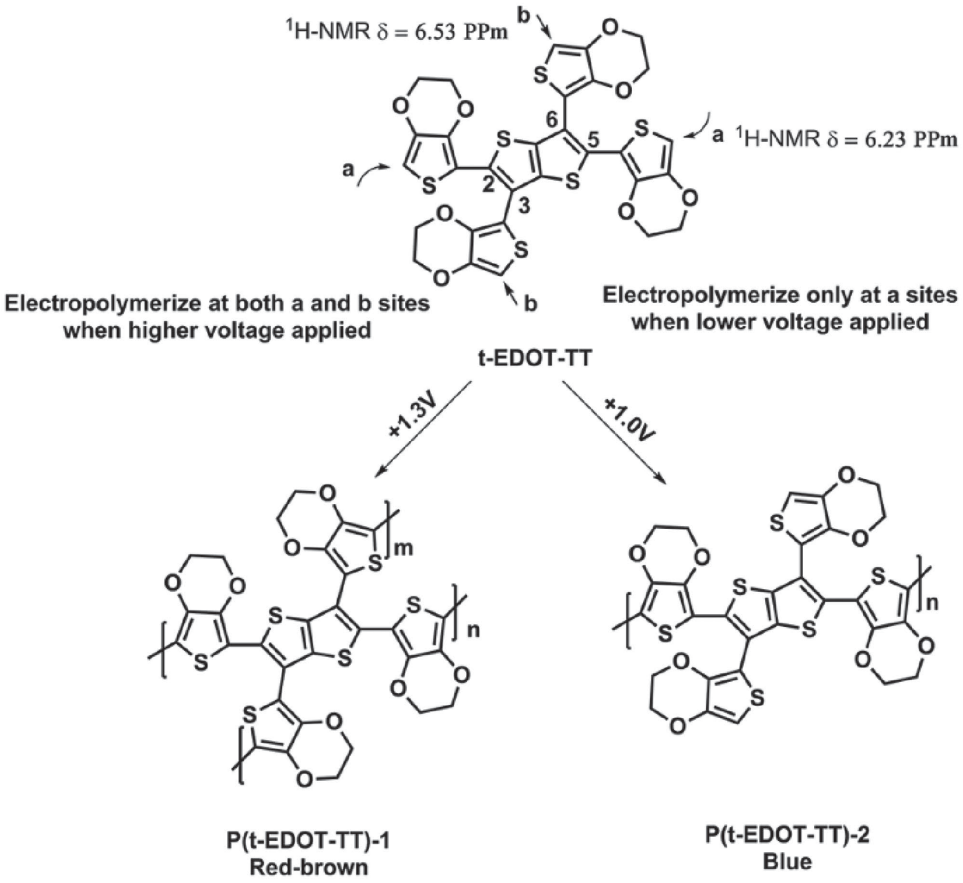

Scheme 2. Electropolymerization process of t-EDOT-TT at two different sites, a and b, controlled by the applied potential, to form P(t-EDOT-TT)-1 and P(t-EDOT-TT)-2.

first cycle of CV, irreversible monomer oxidation peaks were recorded. After successive cycles, formation of new reversible redox couples with an increasing current intensity was observed which proves the deposition of electroactive polymer films on ITO surface.

The inset in Figure 2 shows the photographs of the deposited thin films. The cyclic voltammograms shown in Figure 2 clearly indicate the redox mechanism due to doping and undoping. The first peak oxidation potential of P(t-EDOT-TT)-1 appears at 0.61 V and the first peak reduction potential appears at 0.58 V, at the scan rate of 100 mV s^{-1}. Whereas, for P(t-EDOT-TT)-2, the first peaks of oxidation and reduction potential appear at 0.12 and 0.11 V, respectively, at a scan rate of 100 mV s^{-1}. The lower

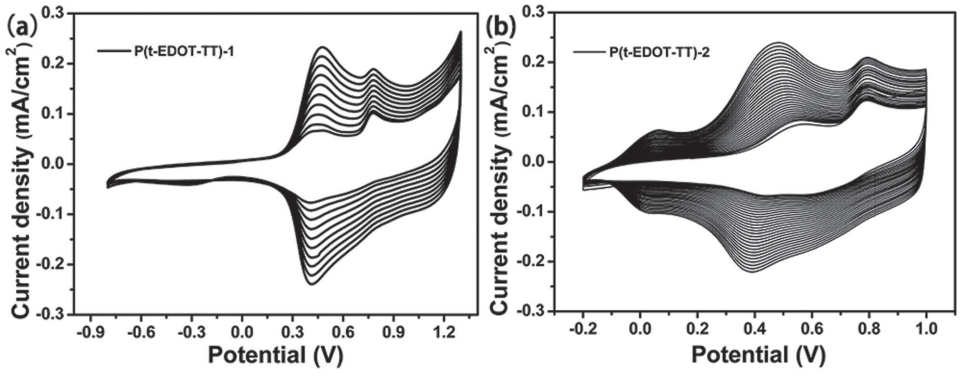

Figure 1. Electrochemical polymerization process of t-EDOT-TT a) formation of P(t-EDOT-TT)-1 at higher applied potential b) formation of P(t-EDOT-TT)-2 at lower potential.

Macromol. Rapid Commun. **2016**, DOI: 10.1002/marc.201600157

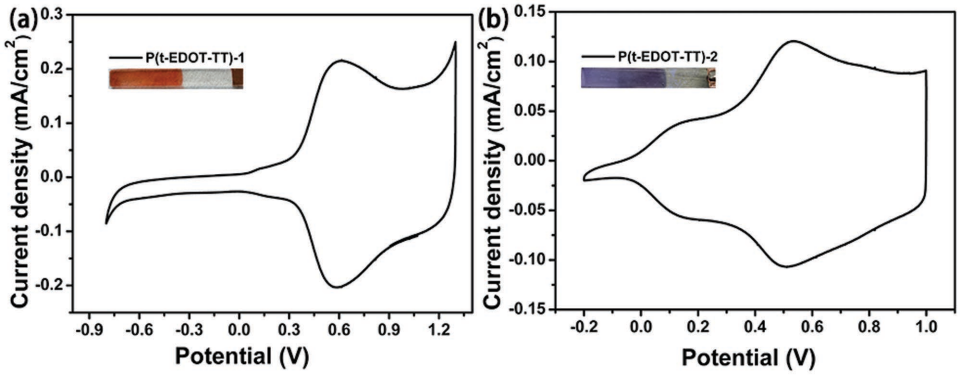

Figure 2. Cyclic voltammetry of P(t-EDOT-TT)-1 and P(t-EDOT-TT)-2. Inset: The thin films of P(t-EDOT-TT)-1 with thickness 150 nm and P(t-EDOT-TT)-2 with thickness 80 nm on ITO coated glass substrate.

oxidation and reduction potential of P(t-EDOT-TT)-2 is attributed to the difference in electron densities of the two reaction sites **a** and **b**.

We performed cyclic voltammetry of the P(t-EDOT-TT) thin films at different scan rates (50, 75, 100, 125, 150, and 200 mV s^{-1}). A dynamic behavior with increasing scan rate was observed and it is obvious from the cyclic voltammograms in Figure 3 that both the P(t-EDOT-TT)-1 and P(t-EDOT-TT)-2 have linear relationship between the current density and scan rate (inset: Figure 3) which shows that the current in polymer thin films is not diffusion controlled. In order to characterize the colors of the synthesized polymers, we measured CIE color coordinates, L*, a*, and b*, where coordinate L* stands for lightness and a* and b* stand for two antagonistic chromatic processes; a* reveals red-green and b* reveals yellow-blue.[24] The corresponding (L*; a*; b*) values for P(t-EDOT-TT)-1 are (63.8; 9.1; 11.3), giving red zone in the neutral state, while that of P(t-EDOT-TT)-2 are (73; −1.3; −4.5), giving blue zone when it is in the neutral state.

While the CVs indicate that the reversible redox processes for both the polymers are plausible, further evidence of electronic transition through oxidation and reduction processes is studied by in situ UV/vis/NIR spectroelectrochemistry (SEC) of the electrochemically deposited thin films on ITO. Figure 4a shows the SEC of 150 nm P(t-EDOT-TT)-1 thin film on the ITO-coated glass substrate. We can see only one absorption band in the visible region and due to the visibility of complementary colors, the device became pinkish-red with the maximum absorption wavelength of λ_{max} = 511 nm at −0.4 V, which is the fully reduced-state of the conducting polymer. With a low applied voltage of +0.5 V, the color of the thin film became brown with maximum absorption wavelength of 489 nm. While at +1.3 V, due to the fully oxidized-states, the device has low absorbance in the visible region and the color seen was light gray. Figure 4b shows the SEC of P(t-EDOT-TT)-2 thin film on the ITO-coated glass substrate. With the maximum absorption wavelength λ_{max} = 604 nm at −0.4 V, the color of the film was blue and with an applied voltage of +0.5 V, the color of the thin film became purple. While at +1.0 V, it turned into light blue color. Figure 4c,d shows the colors of P(t-EDOT-TT)-1 and P(t-EDOT-TT)-2, respectively, at different applied potentials.

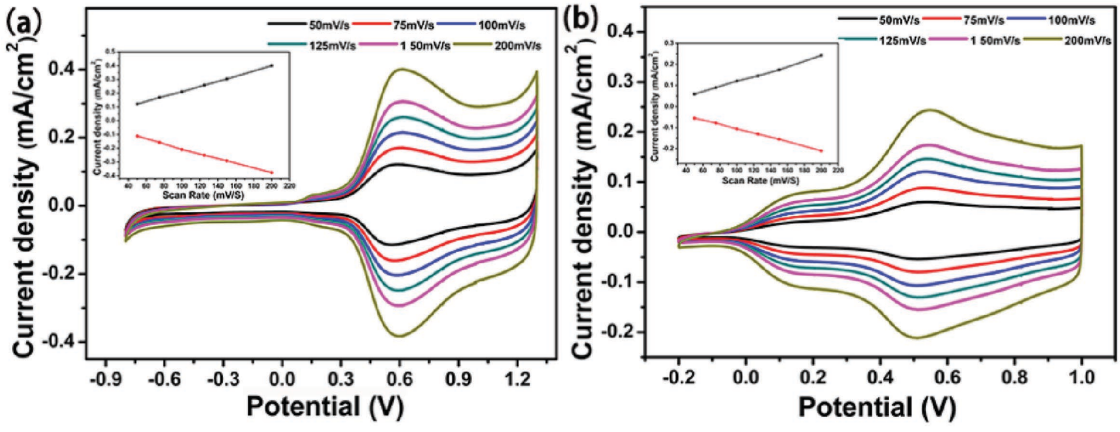

Figure 3. Cyclic voltammetry at the scan rates of 75, 100, 125, 150 mV s^{-1}: a) 150 nm of P(t-EDOT-TT)-1; b) 80 nm of P(t-EDOT-TT)-2. The inset shows linear relationship between current density and scan rate.

Macromolecular Journals
Macromol. Rapid Commun. **2016**, DOI: 10.1002/marc.201600157

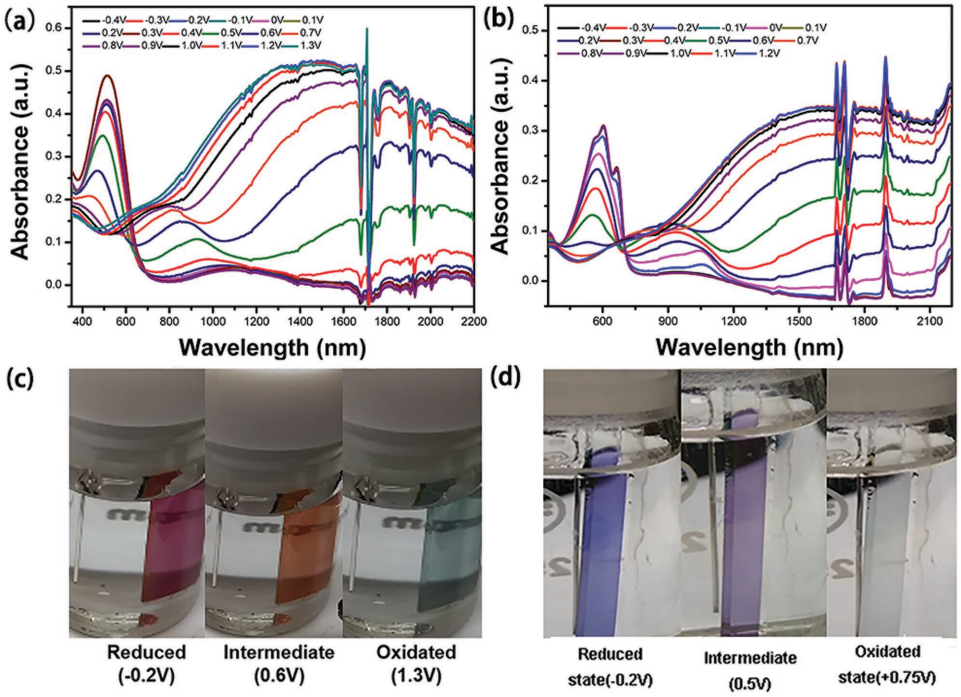

Figure 4. a) Spectroelectrochemistry (SEC) of 150 nm thick P(t-EDOT-TT)-1 on the ITO-coated glass slide in 0.1 M $TBAPF_6$ solution at applied potential range of −0.4 V to +1.3 V; b) SEC of 80 nm thick P(t-EDOT-TT)-2 on the ITO-coated glass slide in 0.1 M $TBAPF_6$ electrolyte solution at applied potential range of −0.4 V to +1.2 V; c) the color change of P(t-EDOT-TT)-1 at different potentials; d) the color change of P(t-EDOT-TT)-1 at different potentials.

At the onset of UV–vis region (698 nm), where π–π* transitions occur, the band gap of P(t-EDOT-TT)-1 was calculated which is equal to 1.78 eV. From the reduction potential to oxidation potential, due to doping, the absorption of the polymer thin film decreases and it becomes almost transparent in the visible region while the residual absorption gives light blue color in the oxidation state. The band gap of P(t-EDOT-TT)-2 as calculated from the UV–vis spectrum is 1.73 eV corresponding to the wave length of 718 nm. Upon oxidation, the absorption at 511 nm decreases and the new absorption bands are formed at about 850 and 1500 nm due to the formation of polarons and bipolarons. The higher band gap of P(t-EDOT-TT)-1 may be attributed to the formation of less conjugated structure as compared to P(t-EDOT-TT)-2.

As shown in Figure 5, the transmittance of the same wavelength changes from highest to lowest as the material transforms from oxidized to reduced state. Plots in Figure 5a,b show transmittance changes of P(t-EDOT-TT)-1 for two different wavelengths of 500 and 1500 nm, respectively. The experiment was carried out by applying stepping potential from −0.4 to +1.3 V with a switching interval of 10 s. In the reduced-state, P(t-EDOT-TT)-1 thin film shows 52% transmittance and in the oxidized state, the transmittance is 74%, thus the optical contrast is %△T = 22% in the visible region when the wavelength is 500 nm (Figure 5a). Under the same condition, the optical contrast is %△T = 75% at 1500 nm (Figure 5b). Figure 5c,d shows the same behavior for P(t-EDOT-TT)-2 thin film at 500 and 1500 nm under the same stepping potential. The optical contrast for the wavelengths of 500 and 1500 nm can be calculated as %△T = 38% (Figure 5c) and %△T = 64% (Figure 5d), respectively. The coloration efficiency is an important factor to monitor the performance of OEC films.[25] It reflects the electrical energy consumption to change the color. The coloration efficiency (CE) of P(t-EDOT-TT)-1 at 500 and 1500 nm is 27.9 and 93 $cm^2\ C^{-1}$, respectively. Whereas P(t-EDOT-TT)-2 has CE values of 148.1 and 234.6 $cm^2\ C^{-1}$ at 560 and 1500 nm, respectively.[26,27] Which shows that the P(t-EDOT-TT)-2 has higher CE.

Switching studies were performed to monitor the optical contrast as a function of time and to calculate the switching time of the polymer at fixed absorption max during stepping potential repeatedly between their neutral and oxidized states. Figure 5e shows that the switching time of P(t-EDOT-TT)-1 is only 0.64 s, which is faster than PEDOT while the switching time of P(t-EDOT-TT)-2 is only 0.36 s (Figure 5f).

To investigate the polymers stability, P(t-EDOT-TT)-2 films were cycled 2000 times between −0.4 V (fully neutral state) and +1.0 V (fully oxidized state) in air (Figure 6), a decrease by lower than 20% for the anodic peak current (i_{pa}) and 26% for cathodic peak current(i_{pc}) is observed,

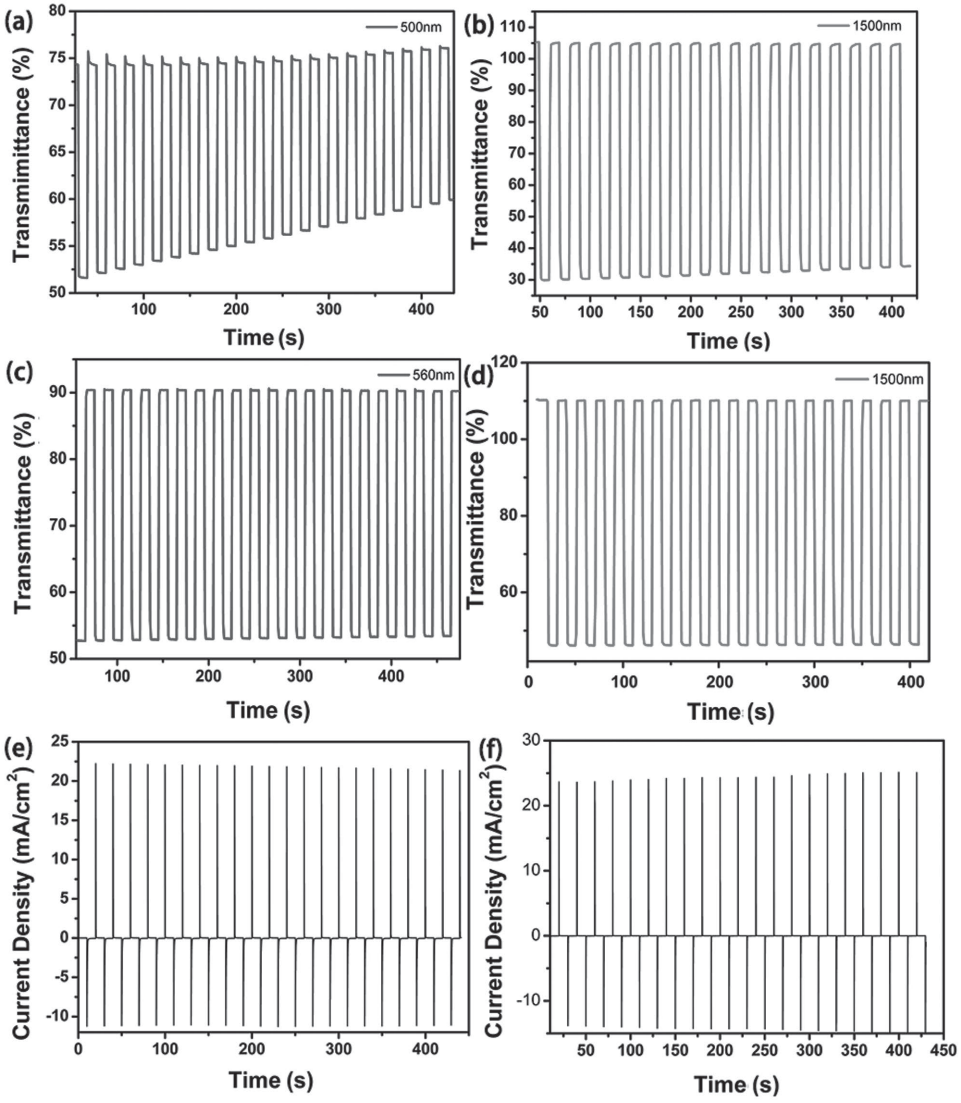

Figure 5. The transmittance of P(t-EDOT-TT) at a) 500 nm of P(t-EDOT-TT)-1; b) 1500 nm of P(t-EDOT-TT)-1; c) 560 nm of P(t-EDOT-TT)-2; d) 1500 nm of P(t-EDOT-TT)-2 current densities versus switching time; e) for P(t-EDOT-TT)-1; f) for P(t-EDOT-TT)-2.

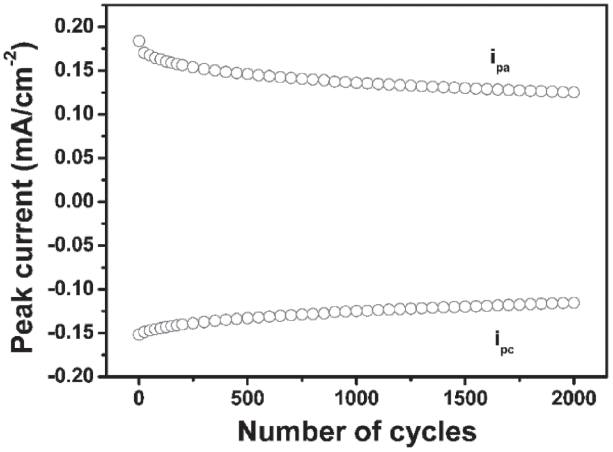

Figure 6. Stability of P(t-EDOT-TT)-2 film cycled 2000 times with a scan rate of 100 mV s^{-1}, in 0.1 M $TBAF_6$/ACN.

showing stability of the films. Moreover, with the increase in the number of cycles, the stability trend is toward a more balanced state.[28]

The optical memory is the propensity of the material to retain its absorption state after removing the external bias.[29,30] The oxidation or reduction bias was applied as a pulse of 2 s, followed by open-circuit condition for 200 s in air. It can be seen, in the optical memory graph of the two polymers in Figure 7, that for P(t-EDOT-TT)-1, there is almost no change in the transmittance when fully reduced state voltage (–0.4 V) is applied after 200 s. Transmittance is lowered by only 1.8% at +0.8 V and 0.6% change at fully oxidized state (+1.3 V) is observed. Similarly for the P(t-EDOT-TT)-2, there is almost no change at fully reduced state voltage (–0.4 V), while 1.3% change at +0.8 V and 1.5% change at fully oxidized state (+1.0 V) is

Macromol. Rapid Commun. **2016**, DOI: 10.1002/marc.201600157

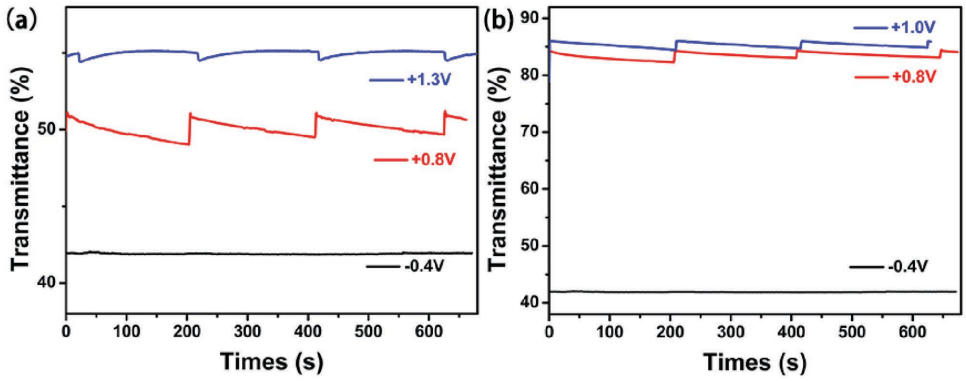

Figure 7. Optical memory of a) P(t-EDOT-TT)-1 polymer at 500 nm; b) P(t-EDOT-TT)-2 polymer at 560 nm.

observed. From the obtained data, we can deduce that both the polymers have reasonable optical memory.

Figure 8 shows atomic force microscopy (AFM) and scanning electron microscope (SEM) images of P(t-EDOT-TT)-1 and P(t-EDOT-TT)-2. Interestingly, the morphology of P(t-EDOT-TT)-1 has a sphere like condensed structure which indicates cross linking in the polymer chains (Figure 8a). We can clearly observe the agglomeration of spherical particles in the SEM image (Figure 8a*). Whereas the AFM image of P(t-EDOT-TT)-2 shows a more layered structure which means that it is 2D as compared to the 3D structure of P(t-EDOT-TT)-1. The SEM image shown in Figure 8b* also confirms the layered structure of P(t-EDOT-TT)-2. Thus, 2,5,3,6 polymerization in the polymer P(t-EDOT-TT)-1 breaks the conjugation and compels the polymer to form 3D structure as compared to the more conjugated and 2D structure of the polymer P(t-EDOT-TT)-2, which is 2,5 polymerized.

Figure 9 shows fourier transform infrared spectrum (FT-IR) of the monomer, P(t-EDOT-TT)-1 and P(t-EDOT-TT)-2. It is clear that the transmittance peaks ascribed to the C—H bending mode from 962 to 700 cm^{-1} reduced dramatically in both polymers, and C—C stretching modes in the range from 1389 to 1340 cm^{-1} appear in the polymer spectra, demonstrating the formation of polymer chains. From the overlap of FT-IR spectra of both the polymers, P(t-EDOT-TT)-1 shows a relatively stronger peak appearing at 1385 cm^{-1}, (arrow a), which is attributed to the C—C bonding modes. However, P(t-EDOT-TT)-2 shows a more broad intense peak at 945 cm^{-1}, (arrow b), which is

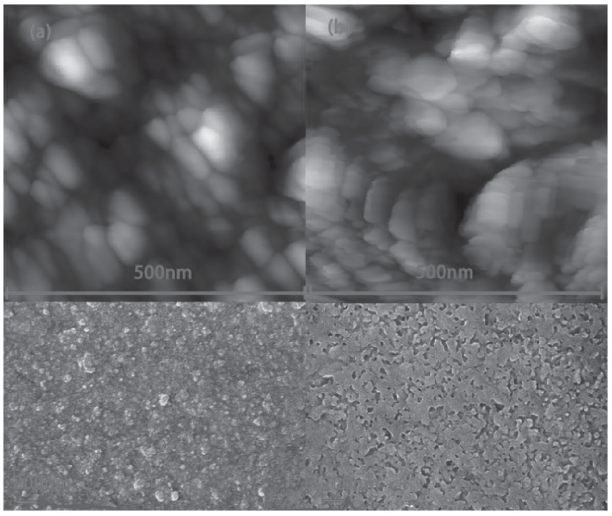

Figure 8. AFM and SEM images of a and a*) P(t-EDOT-TT)-1 and b and b*) P(t-EDOT-TT)-2, respectively.

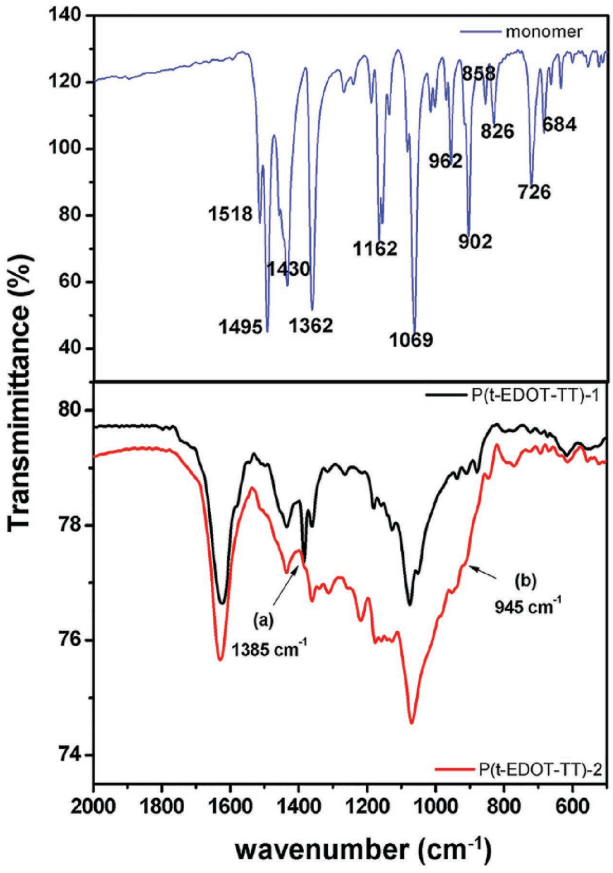

Figure 9. FT-IR spectra of the monomer, P(t-EDOT-TT)-1 and P(t-EDOT-TT)-2.

Macromol. Rapid Commun. **2016**, DOI: 10.1002/marc.201600157

due to the C—H vibration modes of 3,6 substituted EDOT. The rest of the peaks appearing in both the polymers at 1389—1348, 1287, 1510, 1080–1186, and 1415–1440 cm^{-1} are assigned to C–C, C=C, CO–CH_2–CH_2–CO (side chain of EDOT), and C–S bonding, respectively. The peak appearing at 1650 cm^{-1} is because of the electrolyte $TABPF_6$ which is not present in monomer.

4. Conclusions

In conclusion, the synthesis and the electrochromic properties of the butterfly-shaped, tetra-EDOT substituted thieno[3,2-*b*]thiophene material are investigated. Depending on the applied oxidation potential, this new monomer can be reversible modulated to generate two different electrochromic polymers with rapid color switching rates, good reversibility, stability, and reasonable optical memory. Such unique behaviors are attributed to the variable oxidation redox potential feature of thieno[3,2-*b*]-thiophene substituted with EDOT at different positions resulting in the formation of 2D and 3D structures. We envisioned that the approach could be considered as new concept route to develop new redox molecules for future organic electronics applications.

Supporting Information

Supporting Information is available from the Wiley Online Library or from the author.

Acknowledgements: This work was supported by Shenzhen Key Laboratory of Organic Optoelectromagnetic Functional Materials of Shenzhen Science and Technology Plan (ZDSYS20140509094114164), Guangdong Talents Project, Guangdong Natural Science Foundation (2014A030313800), the key materials of OLED application engineering center (KC2015ZDYF0016A), and Shenzhen peacock plan (KQTD2014062714543296), Shenzhen Science and Technology Research Grant (JCYJ20140509093817690), Guangdong Key Research Project (Nos. 2014B090914003, 2015B090914002), National Basic Research Program of China (973 Program, No. 2015CB856505), NSFC (51373075).

Received: March 14, 2016; Revised: May 9, 2016; Published online: ; DOI: 10.1002/marc.201600157

Keywords: 2D-like and 3D-like structures; electrochromism; thieno[3,2-*b*]thiophene; butterfly-shaped compounds

[1] S. K. Deb, J. A. Chopoorian, *J. Appl. Phys.* **1966**, *37*, 4818.
[2] H. Shirakawa, E. J. Louis, A. G. MacDiarmid, C. K. Chiang, A. J. Heeger, *J. Chem. Soc., Chem. Commun.* **1977**, *578*.
[3] C. M. Amb, A. L. Dyer, J. R. Reynolds, *Chem. Mater.* **2011**, *23*, 397.
[4] G. Sonmez, H. Meng, F. Wudl, *Chem. Mater.* **2004**, *16*, 574.
[5] T. T. Steckler, P. Henriksson, S. Mollinger, A. Lundin, A. Salleo, M. R. Andersson, *J. Am. Chem. Soc.* **2014**, *136*, 1190.
[6] K. Li, Q. Zhang, H. Wang, Y. Li, *ACS Appl. Mater. Interfaces* **2014**, *6*, 13043.
[7] H. C. Moon, T. P. Lodge, C. D. Frisbie, *Chem. Mater.* **2015**, *27*, 1420.
[8] P. Barbosa, L. Rodrigues, M. Silva, M. Smith, A. Goncalves, E. Fortunato, *J. Mater. Chem.* **2010**, *20*, 723.
[9] W. Yuan, N. Zhou, L. Shi, K.-Q. Zhang, *ACS Appl. Mater. Interfaces* **2015**, *7*, 14064.
[10] A. M. Österholm, D. E. Shen, J. A. Kerszulis, R. H. Bulloch, M. Kuepfert, A. L. Dyer, J. R. Reynolds, *ACS Appl. Mater. Interfaces* **2015**, *7*, 1413.
[11] S. Lehtimäki, M. Suominen, P. Damlin, S. Tuukkanen, C. Kvarnström, D. Lupo, *ACS Appl. Mater. Interfaces* **2015**, *7*, 22137.
[12] G. Sonmez, H. B. Sonmez, *J. Mater. Chem.* **2006**, *16*, 2473.
[13] R. J. Mortimer, *Annu. Rev. Mater. Res.* **2011**, *41*, 241.
[14] G. Sonmez, C. K. F. Shen, Y. Rubin, F. Wudl, *Angew. Chem.* **2004**, *116*, 1524.
[15] Y. Yuan, G. Giri, A. L. Ayzner, A. P. Zoombelt, S. C. B. Mannsfeld, J. Chen, D. Nordlund, M. F. Toney, J. Huang, Z. Bao, *Nat. Commun.* **2014**, *5*, 3005.
[16] J.-I. Park, J. W. Chung, J.-Y. Kim, J. Lee, J. Y. Jung, B. Koo, B.-L. Lee, S. W. Lee, Y. W. Jin, S. Y. Lee, *J. Am. Chem. Soc.* **2015**, *137*, 12175.
[17] Y. Wang, S. Zou, J. Gao, H. Zhang, G. Lai, C. Yang, H. Xie, R. Fang, H. Li, W. Hu, *Chem. Commun.* **2015**, *51*, 11961.
[18] M. Turbiez, N. Hergué, P. Leriche, P. Frère, *Tetrahedron Lett.* **2009**, *50*, 7148.
[19] Y. Liu, Q. Liu, X. Zhang, L. Ai, Y. Wang, R. Peng, Z. Ge, *New J. Chem.* **2013**, *37*, 1189.
[20] G. E. Gunbas, A. Durmus, L. Toppare, *Adv. Funct. Mater.* **2008**, *18*, 2026.
[21] D. Mo, S. Zhen, J. Xu, W. Zhou, B. Lu, G. Zhang, Z. Wang, S. Zhang, Z. Feng, *Synth. Met.* **2014**, *198*, 19.
[22] B. Lu, S. Zhen, S. Zhang, J. Xu, G. Zhao, *Poly. Chem.* **2014**, *5*, 4896.
[23] G. A. Sotzing, J. L. Reddinger, A. R. Katritzky, J. Soloducho, R. Musgrave, J. R. Reynolds, P. J. Steel, *Chem. Mater.* **1997**, *9*, 1578.
[24] R. C. Silva, M. V. Sarmento, F. A. R. Nogueira, J. Tonholo, R. J. Mortimer, R. Faez, A. S. Ribeiro, *RSC Adv.* **2014**, *4*, 14948.
[25] H. Kim, Y. Park, D. Choi, S.-H. Ahn, C. S. Lee, *Appl. Surf. Sci.* **2016**, *377*, 370.
[26] S. Ming, S. Zhen, K. Lin, L. Zhao, J. Xu, B. Lu, *ACS Appl. Mater. Interfaces* **2015**, *7*, 11089.
[27] S. Zhen, J. Xu, B. Lu, S. Zhang, L. Zhao, J. Li, *Electrochim. Acta* **2014**, *146*, 666.
[28] K. Lin, S. Zhen, S. Ming, J. Xu, B. Lu, *New. J. Chem.* **2015**, *39*, 2096.
[29] P. M. Beaujuge, J. R. Reynolds, *Chem. Rev.* **2010**, *110*, 268.
[30] E. Rustamlı, S. Goker, S. Tarkuc, Y. A. Udum, L. Toppare, *J. Electrochem. Soc.* **2015**, *162*, 75.